J Supercond Nov Magn (2013) 26:861–865
DOI 10.1007/s10948-012-2026-y

ORIGINAL PAPER

On the Effect of Carbon Nano-Tubes Addition on Structure and Superconducting Properties of Bi(Pb)-2223 Phase

A. Saoudel · A. Amira · Y. Boudjadja · L. Amirouche · N. Mahamdioua · A. Varilci · S.P. Altintas · C. Terzioglu

Received: 5 November 2012 / Accepted: 1 December 2012 / Published online: 29 December 2012

Abstract In this work, a series of ceramic samples of $Bi_{1.6}Pb_{0.4}Sr_2Ca_2Cu_3O_y$ (Bi(Pb)-2223) added with different amounts (0, 0.2 and 0.4 wt%) of carbon nano-tubes (*CNT*) are prepared from commercial powders and characterized. The study shows that the volume fraction of the Bi(Pb)-2223 phase decreases with *CNT* content while the grain size of the samples increases. The obtained cell parameters as well as the onset critical transition temperature are independent of this kind of addition. Also, it has been concluded that *CNT* addition makes the grains of the samples more connected. The measured magnetization in FC and ZFC modes indicates that *CNT* addition makes the grains of the samples more connected even if the irreversibility line is decreased. The variation of the residual resistivity and metallicity with *CNT* content suggests that the addition introduces disorder and defects into the samples. Also, the added samples present broad transitions to the superconducting state when compared to the pure one; this result may be associated to the increase of the volume fraction of the secondary phases. The activation energies, upper critical fields $H_{c2}(0)$ and coherence lengths $\xi(0)$ are extracted from the magnetoresistivity curves and their evolutions with *CNT* content are discussed.

Keywords Bi-2223 phase · Structure · Activation energy · Electrical and magnetic properties

A. Saoudel (✉) · A. Amira · Y. Boudjadja · L. Amirouche · N. Mahamdioua
LEND, Faculty of Science and Technology, Jijel University, 18000 Jijel, Algeria
e-mail: dca.saoudel@yahoo.fr

N. Mahamdioua · A. Varilci · S.P. Altintas · C. Terzioglu
Department of Physics, Faculty of Arts and Sciences, AIB University, 14280 Bolu, Turkey

1 Introduction

The Bi(Pb)-2223 superconductors are very promising for future applications because of their high critical temperature and critical current density. In the recent years, various kinds of doping have been employed to improve the properties of cuprates by including carbon nanotubes, SiC, B_4C and various carbon sources [1–4]. However, only very limited effort has been devoted to the flux pinning and grain coupling of the Bi(Pb)-2223 bulk materials. Also, few researches were carried out on the Carbon Nanotubes (CNT) addition in cuprates. This work concerned only the Y-123 and Bi(Pb)-2212 phases [1, 3].

In a way to improve the interconnectivity, flux pinning and the volume fraction, a lot of attention is currently given for additions of different compounds in Bi(Pb)-2223 [5–7]. However, this enhancement is not obtained for all addition compounds [8, 9].

To the best of our knowledge, carbon CNT additions in Bi(Pb)-2223 superconductors have not yet been reported. Aiming to test the effect of this kind of addition on properties of this phase, series with different amounts of CNT are prepared and characterized. The results are discussed by a correlation between the different studies.

2 Experimental

A bismuth-based powder (ALDRICH) with chemical formula $Bi_{1.6}Pb_{0.4}Sr_2Ca_2Cu_3O_y$ was mixed with different amounts (0, 0.2 and 0.4 wt.%) of carbon nano-tubes (ALDRICH) of about 30 nm of size. Hereafter, the samples will be called CNT00, CNT02 and CNT04 for $x = 0, 0.2$ and 0.4 wt.%, respectively. The powders are hand milled and pressed into pellets which have been sintered at 850 °C in air

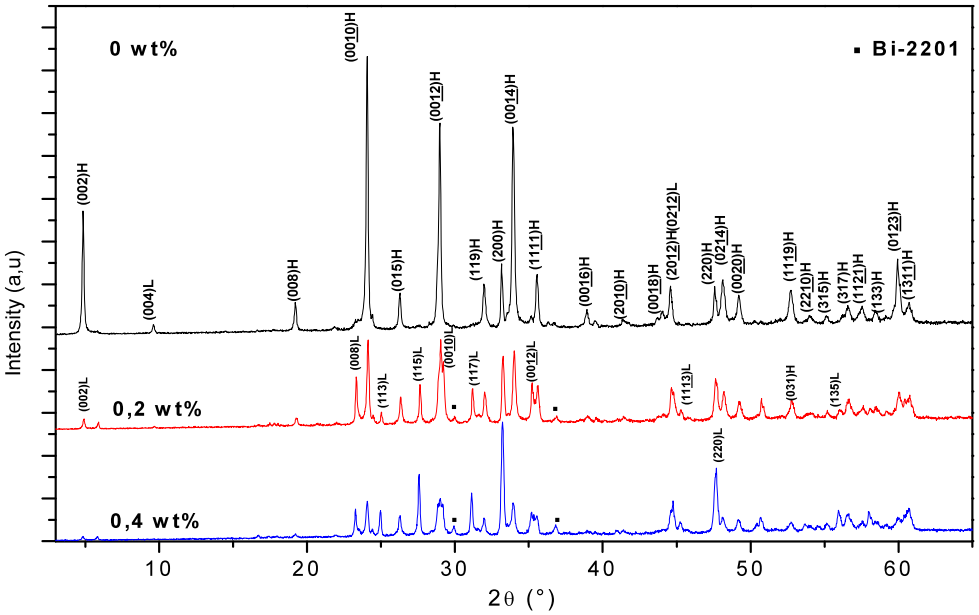

Fig. 1 XRD patterns of CNT added $Bi_{1.6}Pb_{0.4}Sr_2Ca_2Cu_3O_y$ samples

during 20 h. The samples are characterized by X-ray diffraction (Siemens D8-Advance powder diffractometer), scanning electron microscopy (JEOL JSM-6390LV microscope), electrical resistivity (Cryodine CTI-Cryogenics closed cycle cryostat) and magnetization measurements (PPMS magnetometer).

3 Results and Discussion

Figure 1 shows the XRD patterns of the samples. They consist of Bi(Pb)-2223 and Bi(Pb)-2212 phases. The lines belonging to these two phases are indexed by the letters H and L, respectively. For CNT00 sample, the obtained high intensities of *(0010)*, *(0012)* and *(0014)* lines of Bi(Pb)-2223 phase attests of a texture along the *(00l)* direction. However, it is not the case for CNT02 and CNT04 samples. In addition to these two main phases, extra small lines belonging to Bi-2201 phase (JCPDS 46-0392 file) are marked by the ■ symbol. The cell parameters are calculated by use of JANA2006 software [10]. The refinement is carried out simultaneously in the orthorhombic system with the *A2aa* and *Bbmb* space groups for Bi(Pb)-2223 and Bi(Pb)-2212 phases, respectively [11–13]. The obtained cell parameters as well as the refinement factors (R_p, R_{wp}, GOF) are listed in Table 1. Since the addition does not have any significant effect on the values of cell parameters, CNT could then be introduced as interstitial and not substitutional. This result is similar to that reported by Dadras et al. [1] for Y-123 compounds. The relative volume fraction f_{2223} of the Bi(Pb)-2223 phase is calculated from the peaks intensities of the observed lines [11, 14, 15]. As is shown in Table 1, the CNT00 sample shows the highest proportion (94.98 %). This fraction decreases by CNT addition similarly to that reported for Gd added Bi(Pb)-2223 phase [16].

As shown in Fig. 2, the addition of CNT increases the grain size of the samples. CNT02 sample appears to have better grain connection when compared to others. For CNT04, large plate-like grains with a random distribution are formed with a clear porosity. This result could be due to the reduction of the melting temperature by CNT addition [11].

The temperature dependence of magnetization in FC and ZFC modes is displayed in Fig. 3. The onset critical transition temperature seems to be independent of CNT addition, in agreement with the reported results for Bi(Pb)-2212 phase [3]. This result may be explained by the fact that CNT are located in the grain boundaries [3] of the samples and do not affect the charge carriers density of the CuO_2 planes. The highest Meissner signal and thus the effective superconducting volume fraction is observed for the pure CNT00 sample. This result may be due to the high volume fraction of Bi(Pb)-2223 phase seen for this sample [11]. It is also remarkable that the transition is very broad for CNT02 and CNT04 samples. The difference of magnetizations ΔM of the FC and ZFC modes are about 8.178×10^{-3}, 1.102×10^{-3} and 5.846×10^{-3} emu/g at 10 K for CNT00, CNT02 and CNT04 samples, respectively. The smallest value of ΔM seen for CNT02 sample attests of a better connection of its grains [17]. This result is in good agreement with the SEM analysis.

The magneto-resistivity measurements of the samples under different magnetic field up to 3 T are shown in Fig. 4. The transition width increases with increasing applied magnetic field and CNT content. Also, the degree of the broad-

Table 1 Cell parameters (a, b, c, V), agreement factors (R_p, R_{wp}, GOF), volume fraction f_{2223} of Bi(Pb)-2223 phase, residual resistivity (ρ_0), $H_{c2}(0)$ and $\xi(0)$ values of the samples

x wt%	0	0.2	0.4
a (Å)	5.3997(6)	5.3914(6)	5.3984(5)
b (Å)	5.4059(6)	5.4033(4)	5.4107(6)
c (Å)	37.0031(8)	36.983(1)	36.985(1)
V (Å^3)	1080.14(8)	1076.7(1)	1080.3(1)
$(R_p, R_{wp})\%$	(7.11, 10.40)	(7.68, 10.99)	(7.19, 10.27)
GOF	1.93	1.86	1.63
f_{2223} (%)	94.98	63.94	55.89
ρ_0 (Ω cm)	1.976×10^{-5}	6.48×10^{-3}	1.071×10^{-2}
$H_{C2}(0)$ (T)	232.190	246.103	231.859
$\xi(0)$ (Å)	11.906	11.565	11.915

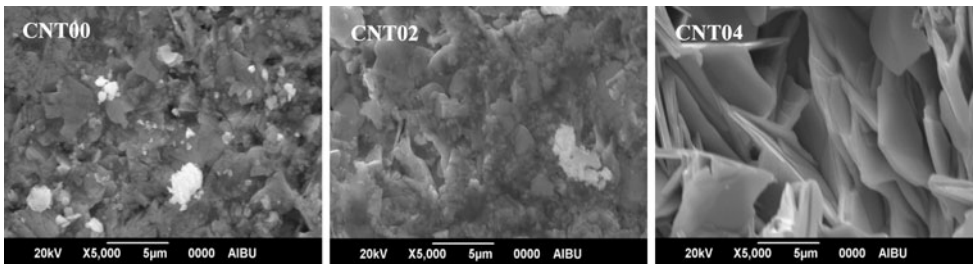

Fig. 2 SEM photographs of CNT added $Bi_{1.6}Pb_{0.4}Sr_2Ca_2Cu_3O_y$ samples

ening for CNT00 sample is less than those of CNT02 and CNT04 samples. The large broadening of the resistive transition in magnetic field is a direct consequence of thermal fluctuations in the vortex system. Also T_c offset values decrease significantly by applying the magnetic field and CNT addition. The grains of the added samples are then less homogeneous as well as the applied magnetic field mostly affects the inter-granular coupling [18]. Also, the presence of the Bi(Pb)-2212 secondary phase affects and widens the superconductive transition [11]. We believe that the double step resistive transition is a confirmation of the existence of this secondary phase which plays the role of the weak links at the grain boundaries [19]. As seen in Table 1, the residual resistivity ρ_0 increases with increasing CNT addition, suggesting that the added samples are more disordered than the pure one [11, 20]. The slope $d(\rho)/dT$ of the linear part of the normal state region is about 7.14×10^{-3}, 1.68×10^{-3} and 3.26×10^{-4} K^{-1} for $x = 0, 0.2$ and 0.4, respectively. This slope may be considered as a parameter that depends on the intrinsic electronic interactions that affect the transport properties [12]. Its decrease with CNT addition agrees well with the variation of the residual resistivity and confirms the introduced disorder into the samples. The tail part of resistivity has been found to follow Arrhenius relation as given by $\rho(H, T) = A \exp(-U_0/k_B T)$ [6]. Here A is the pre-exponent factor, k_B the Boltzmann constant and U_0 is the activation energy for the flux motion.

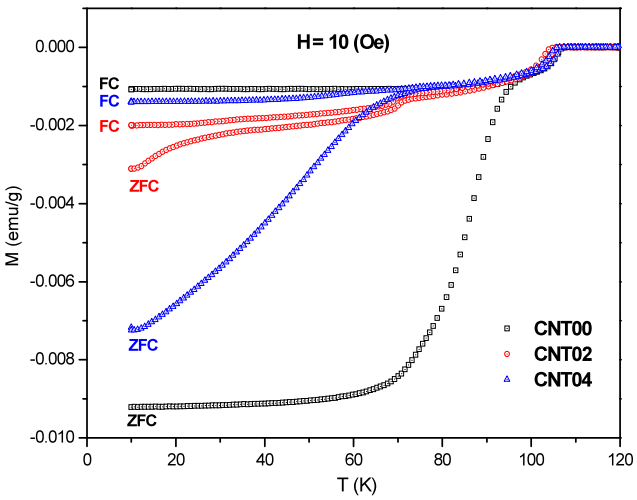

Fig. 3 FC and ZFC magnetizations of CNT added $Bi_{1.6}Pb_{0.4}Sr_2Ca_2Cu_3O_y$ samples

U_0 is expected to give information about the mechanism of dissipation and can be directly calculated from the slop of linear part of plot of $\ln(\rho/\rho_0)$ versus $1/T$. The estimated values of U_0 are given in Fig. 5. The activation energy decreases significantly by increasing the amount of CNT addition and applied magnetic field, indicating the thermal activation dissipation behavior in the Bi(Pb)-2223 system. It seems that the values of U_0 are stabilized for high field.

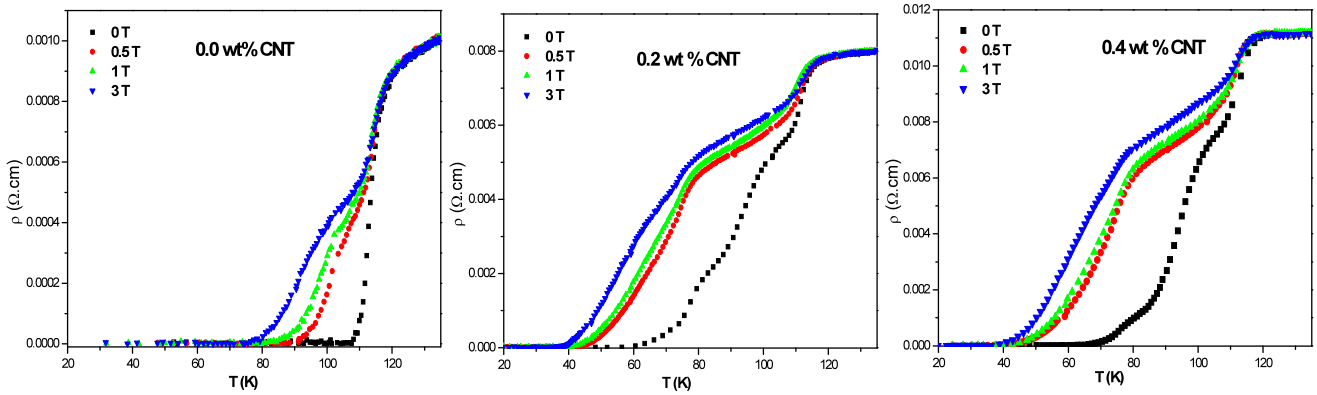

Fig. 4 Temperature dependence of resistivity of CNT added $Bi_{1.6}Pb_{0.4}Sr_2Ca_2Cu_3O_y$ samples

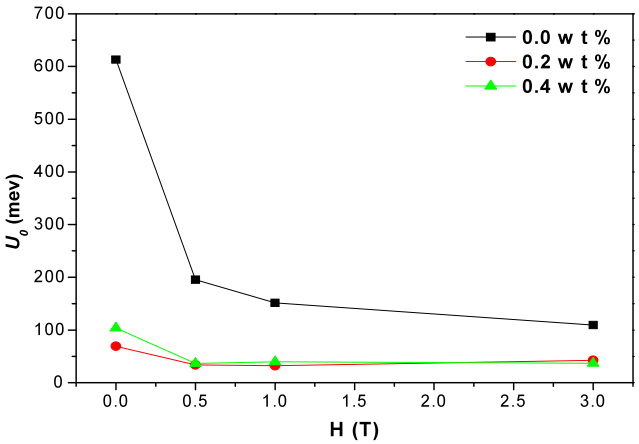

Fig. 5 The activation energy (U_0) versus magnetic field for the samples

A similar result was reported by Abbasi et al. [8] in $MgCO_3$ added Bi(Pb)-2223 phase.

The upper critical field H_{c2} of the samples could be estimated from the temperature dependence of resistivity at $\rho(H_{c2}, T) = 0.9\rho_n$, where ρ_n is the normal state resistivity at the onset critical transition temperature $T_{c.on}$ [21]. As is shown in Table 1, the $H_{c2}(0)$ values increase from 232.19 T for the pure CNT00 sample to 246.103 T for the CNT02 sample and for high amount of CNT (0.4 wt%), it decreases to 231.859 T. Similar results for $H_{c2}(0)$ values have been reported by Yildirim et al. [22].

In order to approximate the superconducting parameters, we have used the Ginzburg-Landau formula for estimation of the coherence length (ξ) [9]. Table 1 gives the estimated values of $\xi(0)$ at zero temperature. The best value is seen for CNT02 sample (11.56 Å) and increases slightly (11.91 Å) for CNT04. This suggests that the non-superconducting regions increase with this kind of addition. These results are similar to those reported by several author [6, 8, 9] in samples added with different compounds. Finally, it is noted from Table 1 that the values of $\xi(0)$ and $H_{c2}(0)$ prove an inverse behavior that confirms the good correlation between them.

4 Conclusion

We have shown that the addition of carbon nano-tubes to $Bi_{1.6}Pb_{0.4}Sr_2Ca_2Cu_3O_y$ superconductors does not affect the cell parameters and onset T_c, decreases the volume fraction of the Bi(Pb)-2223 phase and activation energy, increases the grain size of the samples and the coherence length, makes the grains more connected, and improves the upper critical field .

References

1. Dadras, S., Liu, Y., Chai, Y.S., Daadmehr, V., Kim, K.H.: Physica C **469**, 55–59 (2009)
2. Galvan, D.H., Li, S., Yuhasz, W.M., Kim, J.H., Maple, M.B., Adem, E.: Physica C **403**, 145–150 (2004)
3. Galvan, D.H., Durán, A., Castillón, F.F., Adem, E., Escudero, R., Ferrer, D., Torres, A., José-Yacamán, M.: J. Supercond. Nov. Magn. **21**, 271–277 (2008)
4. Yang, Z.Q., Su, X.D., Qiao, G.W., Guo, Y.C., Dou, S.X., de Boer, F.R.: Physica C **325**, 136–142 (1999)
5. Gul, I.H., Amin, F., Abbasi, A.Z., Anis-ur-Rehman, M., Maqsood, A.: Physica C **449**, 139–147 (2006)
6. Abbasi, H., Taghipour, J., Sedghi, H.: J. Alloys Compd. **494**, 305–308 (2010)
7. Mikhailov, B.P., Rudnev, I.A., Bobin, P.V., Kadyrbaev, A.R., Mikhailova, A.B., Pokrovskii, S.V.: Izv. Ross. Akad. Nauk Ser. Fiz. **71**, 1145–1149 (2007)
8. Abbasi, H., Taghipour, J., Sedghi, H.: J. Alloys Compd. **482**, 552–555 (2009)
9. Erdem, M., Ozturk, O., Yucel, E., Altintas, S.P., Varilci, A., Terzioglu, C., Belenli, I.: Physica B **406**, 705–709 (2011)
10. Petricek, V., Dusek, M., Palatinus, L.: JANA2006: The Crystallographic Computing System, p. 200. Institute of Physics, Praha (2006)
11. Amira, A., Saoudel, A., Boudjadja, Y., Amirouche, L., Mahamdioua, N., Varilci, A., Akdogan, M., Terzioglu, C., Mosbah, M.F.: Physica C **471**, 1621–1626 (2011)

12. Amira, A., Boudjadja, Y., Saoudel, A., Varilci, A., Akdogan, M., Terzioglu, C., Mosbah, M.F.: Physica B **406**, 1022–1027 (2011)
13. Giannini, E., Gladyshevskii, R., Clayton, N., Musolino, N., Garnier, V., Piriou, A., Flükiger, R.: Curr. Appl. Phys. **8**, 115–119 (2008)
14. Akdogan, M., Terzioglu, C., Varilci, A., Belenli, I.: Physica B **405**, 4010–4019 (2010)
15. Salamati, H., Kameli, P.: Physica C **403**, 60–66 (2004)
16. Terzioglu, C., Aydin, H., Ozturk, O., Bekiroglu, E., Belenli, I.: Physica B **403**, 3354–3359 (2008)
17. Mune, P., Govea-Alcaide, E., Jardim, R.F.: Physica C **384**, 491–500 (2003)
18. Nursoy, M., Yilmazlar, M., Terzioglu, C., Belenli, I.: J. Alloys Compd. **459**, 399–406 (2008)
19. Grinenko, V., Krasnoperov, E.P., Stoliarov, V.A., Bush, A.A., Mikhajlov, B.P.: J. Phys. Conf. Ser. **43**, 492–495 (2006)
20. Pignon, B., Autret-Lambert, C., Ruyter, A., Decourt, R., Bassat, J.M., Monot-Laffez, I., Ammor, L.: Physica C **468**, 865–871 (2008)
21. Kim, J.H., Dou, S.X., Shi, D.Q., Rindfleisch, M., Tomsic, M.: Supercond. Sci. Technol. **20**, 1026–1031 (2007)
22. Yildirim, G., Akdogan, M., Altintas, S.P., Erdem, M., Terzioglu, C., Varilci, A.: Physica B **406**, 1853–1857 (2011)